Supporting Information

Self-Assembly of Single Chain Janus Nanoparticles from Azobenzene-Containing Block Copolymers and Reversible Photoinduced Morphology Transition

Wei Wen,[a] Aihua Chen*,[a,b]

[a] School of Materials Science and Engineering, Beihang University, Beijing 100191, P. R. China
[b] Beijing Advanced Innovation Centre for Biomedical Engineering, Beihang University, Beijing 100191, P. R. China

E-mail: chenaihua@buaa.edu.cn

Characterizations

Bruker DMX Spectrometer (400 MHz) was employed to record ^{1}H NMR spectra using $CDCl_3$ as the solvent. GPC was conducted by using a Waters 2410 GPC equipped with styragel columns. The flow rate of THF (HPLC) eluent is 1 mL/min. A series of monodisperse polystyrene standards was used to calibrate M_n. Transmission electron microscopy (TEM) of JEM-2100 with an accelerating voltage of 200 kV was used to observe the morphologies. The TEM samples were prepared by casting one drop of the diluted dispersion on a carbon-coated copper grid and dried at room temperature. Before observation, the assemblies were stained by RuO_4. Shandong Naikete NKT-N9 instrument equipped with a 532 nm He-Ne laser was used for dynamic light scattering (DLS) measurements at 25 ^{o}C. UV-vis spectra were recorded on a SHIMADZU UV-2600 spectrophotometer. The 360 nm UV and 520 nm visible light, used for studying photo-responsive behavior of assemblies, were produced by OMRON-ZUV-H20MC (~ 25 mW/cm^2) and CCS-PJ-1505-2CA (~ 500 mW/cm^2), respectively. The dimerization degree (= $1 - A_t/A_0$, where A_0 and A_t are the absorbance before and after irradiation for 40 min, respectively) of MAStb groups was calculated using the peak intensity at 310 nm[1-3] and the photoisomerization efficiency (= $1 - A_t/A_0$, where A_0 and A_t are the absorbance before and after irradiation for 40 min, respectively) of azobenzene moieties was calculated using the peak intensity at 375 nm. NETZSCH DSC214 instrument was employed to conduct differential scanning calorimetry (DSC) analyses. The DSC samples were scanned under air flow from 25 ^{o}C to 200 ^{o}C at a heating/cooling rate of ± 10 ^{o}C /min. Shang Guang 59XF microscope equiped with a Shang Guang XRD thermo-control system was used to conduct polarized optical microscopic (POM) observation. Anton-Paar SAXS mc2 diffractometer with Cu Kα radiation was employed to conduct Small-angle Xray scattering (SAXS) measurment. The BCP precursors were annealed at 160 °C for 3 h and then cooled to 140 °C for 24 h under vacuum.

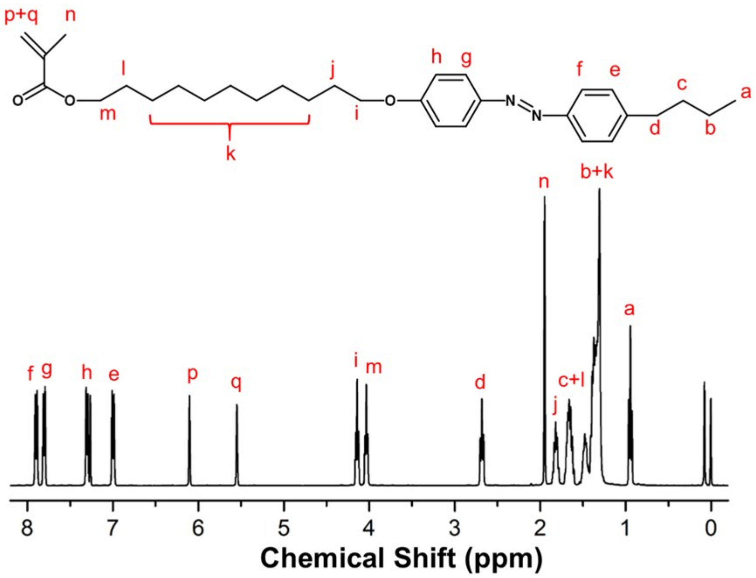

Fig. S1 Chemical structure and ^{1}H NMR spectrum of MAAz monomer.

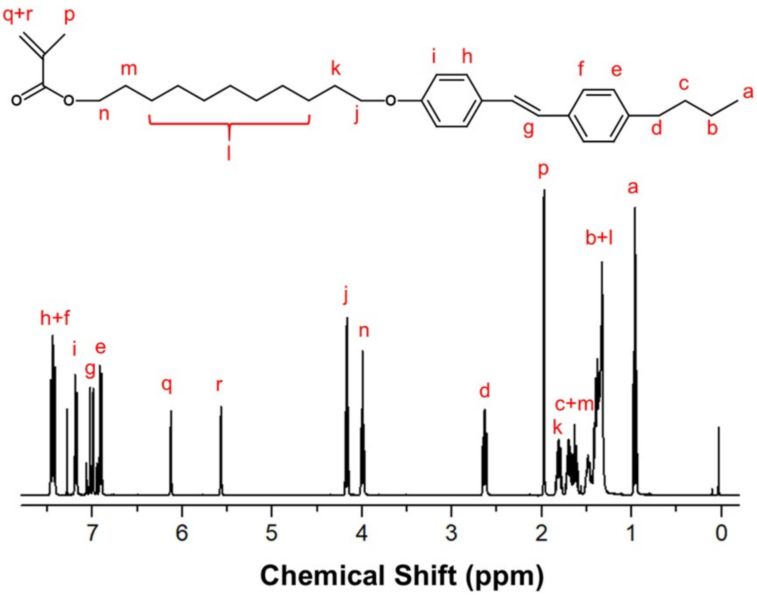

Fig. S2 Chemical structure and ^{1}H NMR spectrum of MAStb monomer.

Table S1. Characterization of BCP precursors and corresponding SCJNPs.

Sample[a]	M_n of BCP (kg/mol)[a]	M_n of BCP (kg/mol)[b]	M_w/M_n of BCP[b]	M_n of SCJNP (kg/mol)[b]	M_w/M_n of SCJNP[b]	f_{PEGMA}[c]	f_{PMAAz}[c]	f_{PMAStb}[c]
PPEGMA$_{14}$-*b*-P(MAAz$_{63}$-*co*-MAStb$_{33}$)	51.3	48.7	1.38	45.3	1.43	8.2	60.3	31.5
PPEGMA$_{14}$-*b*-P(MAAz$_{37}$-*co*-MAStb$_{72}$)	57.6	51.3	1.35	48.9	1.41	7.3	31.5	61.2
PPEGMA$_{31}$-*b*-P(MAAz$_{60}$-*co*-MAStb$_{32}$)	54.5	49.7	1.21	47.4	1.23	17.0	54.2	28.8
PPEGMA$_{31}$-*b*-P(MAAz$_{34}$-*co*-MAStb$_{66}$)	58.3	51.6	1.23	49.1	1.25	15.9	28.7	55.4

[a]The DPs of PMAAz and PMAStb, M_n were calculated from ^{1}H NMR spectra.

[b]The M_n and M_w/M_n values were determined by GPC.

[c]The weight fractions (wt.%) were calculated from ^{1}H NMR results.

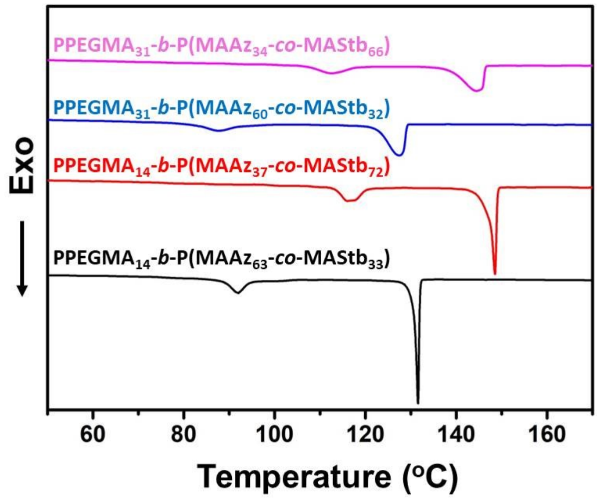

Fig. S3 DSC curves of PPEGMA$_x$-*b*-P(MAAz$_m$-*co*-MAStb$_n$) during the first cooling process.

Table S2. Thermal properties of PPEGMA$_x$-*b*-P(MAAz$_m$-*co*-MAStb$_n$) BCPs and PMAAz, PMAStb homopolymers.

Sample	Transition temperature (^{o}C)	
	$T_{S\text{-}Sm}$[c]	$T_{Sm\text{-}I}$[d]
PMAAz$_{57}$[a]	69.5	117.7
PMAStb$_{31}$[a]	151.1	165.8
PPEGMA$_{14}$-*b*-P(MAAz$_{63}$-*co*-MAStb$_{33}$)[b]	93.3	135.4
PPEGMA$_{14}$-*b*-P(MAAz$_{37}$-*co*-MAStb$_{72}$)[b]	118.2	151.6

[a] Reported by Asaoka et al. Macromolecules 2011, 44, 7645-7658.

[b] Measured by DSC.

[c] S-Sm represents the transition of solid phase to smectic phase.

[d] Sm-I represents the transition of smectic phase to isotropic phase.

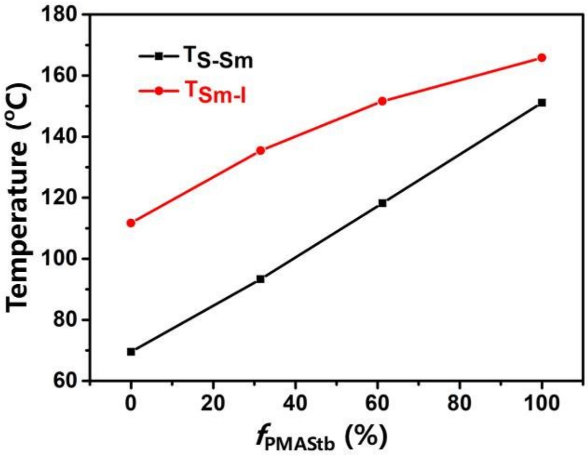

Fig. S4 The plot of transition temperature *vs.* f_{PMAStb}. The data originated from Table S2.

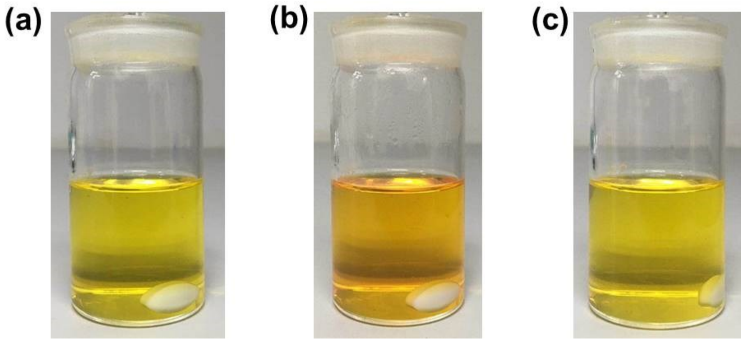

Fig. S5 Photographs of PPEGMA$_{14}$-*b*-P(MAAz$_{63}$-*co*-MAStb$_{33}$) in THF: (a) initial, (b) irradiated with 360 nm UV light for 40 minutes, and (c) subsequently irradiated with 520 nm light for 40 minutes.

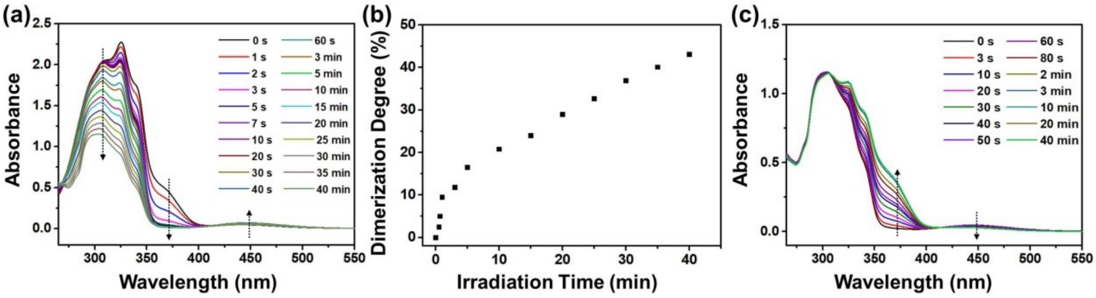

Fig. S6 UV−vis spectra of PPEGMA$_{14}$-*b*-P(MAAz$_{37}$-*co*-MAStb$_{72}$) in THF recorded (a) after different UV irradiation times and (c) after different vis irradiation times. (b) Plot of the photodimerization degree of stilbene *vs.* UV irradiation time. For (c), 0 s is the spectrum after UV irradiation for 40 min.

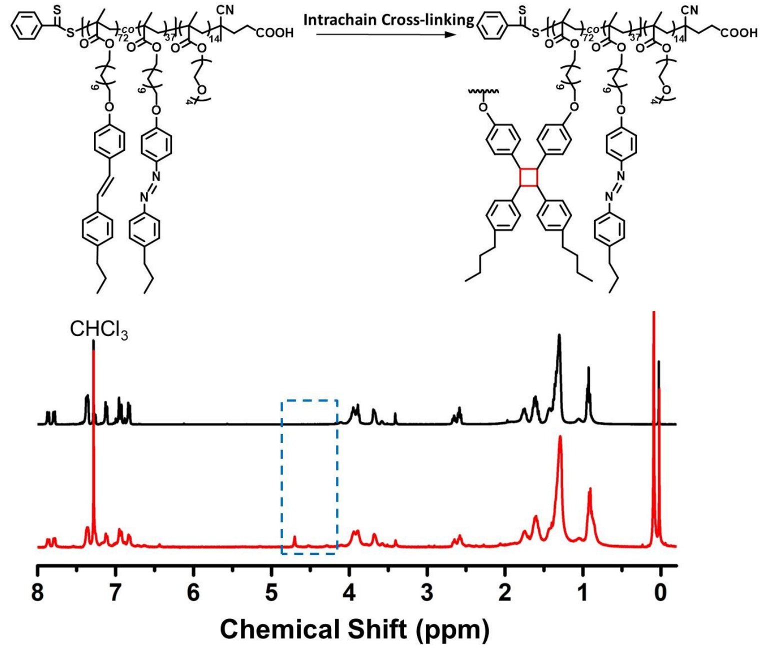

Fig. S7 ^{1}H NMR spectra of PPEGMA$_{14}$-*b*-P(MAAz$_{37}$-*co*-MAStb$_{72}$) before (black line) and after (red line) intrachain cross-linking. Both spectra were recorded in $CDCl_3$.

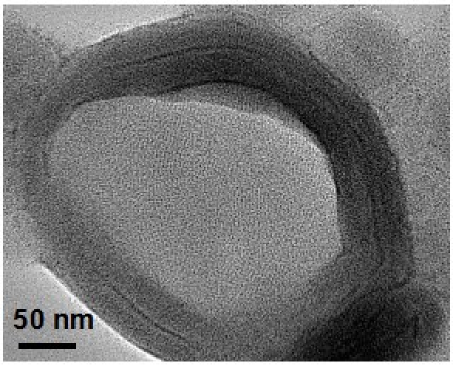

Fig. S8 Magnified TEM image of the assemblies for SCJNPs prepared from PPEGMA$_{14}$-*b*-P(MAAz$_{63}$-*co*-MAStb$_{33}$) with initial concentration of 0.5 wt.%.

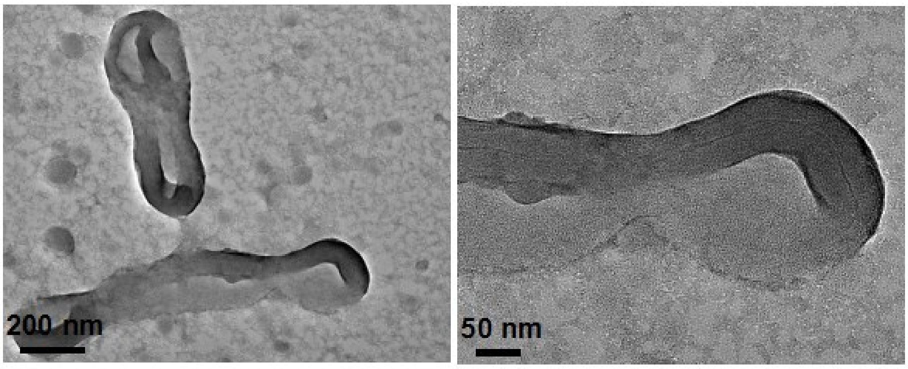

Fig. S9 Magnified TEM images of the assemblies for SCJNPs prepared from PPEGMA$_{14}$-*b*-P(MAAz$_{63}$-*co*-MAStb$_{33}$) with initial concentration of 1.0 wt.%.

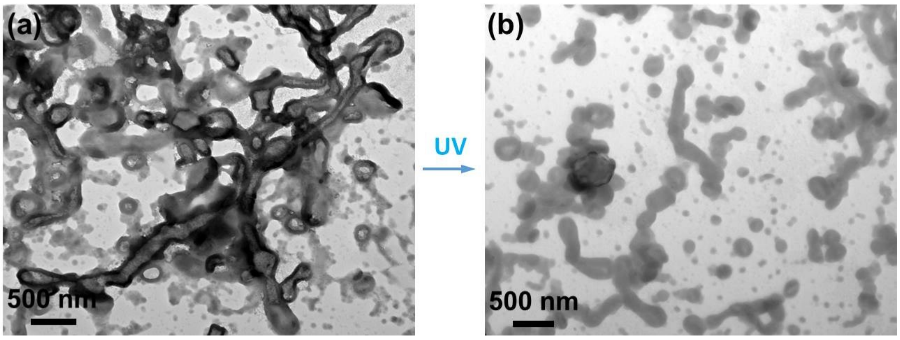

Fig. S10 Representative TEM images of (a) the assemblies for SCJNPs prepared from PPEGMA$_{14}$-*b*-P(MAAz$_{37}$-*co*-MAStb$_{72}$) at initial concentration of 1.0 wt.% and (b) the products after 360 nm UV light irradiation.

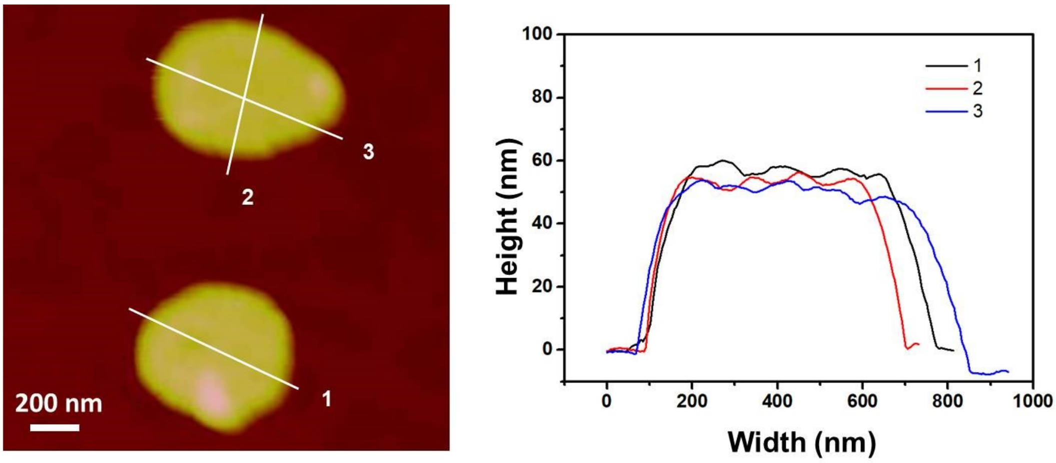

Fig. S11 AFM image and corresponding height profiles of the self-assemblies for SCJNPs prepared from PPEGMA$_{31}$-*b*-P(MAAz$_{34}$-*co*-MAStb$_{66}$) at initial concentration of 1.0 wt.%.

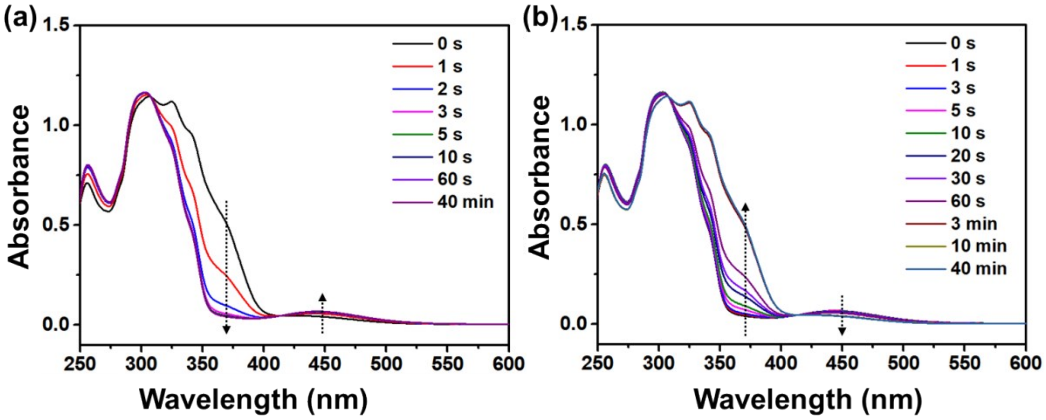

Fig. S12 UV-vis spectra of SCJNPs prepared from PPEGMA$_{14}$-*b*-P(MAAz$_{63}$-*co*-MAStb$_{33}$) in THF with (a) 360 nm UV light irradiation and (b) 520 nm light irradiation. For b, 0 s is the spectrum after irradiation of 360 nm for 40 min.

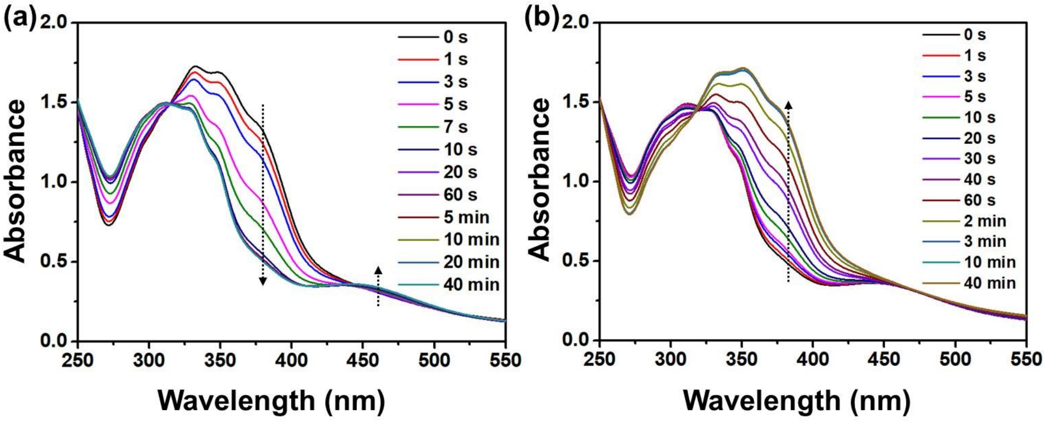

Fig. S13 UV-vis spectra of the assemblies for SCJNPs prepared from PPEGMA$_{31}$-*b*-P(MAAz$_{60}$-*co*-MAStb$_{32}$) in aqueous dispersion irradiated by (a) 360 nm UV light and (b) 520 nm visible light. For (b), 0 s is the spectrum after 360 nm UV irradiation for 40 min.

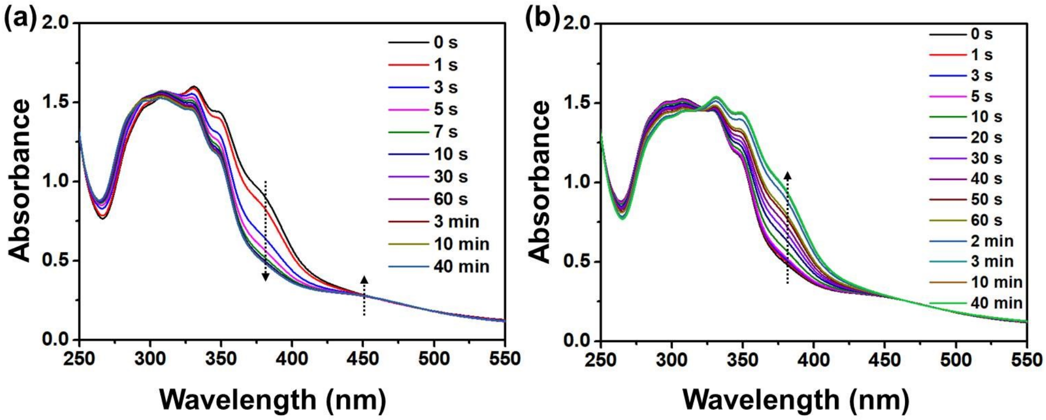

Fig. S14 UV-vis spectra of the assemblies for SCJNPs prepared from PPEGMA$_{31}$-*b*-P(MAAz$_{34}$-*co*-MAStb$_{66}$) in aqueous dispersion irradiated by (a) 360 nm UV light and (b) 520 nm visible light. For (b), 0 s is the spectrum after 360 nm UV irradiation for 40 min.

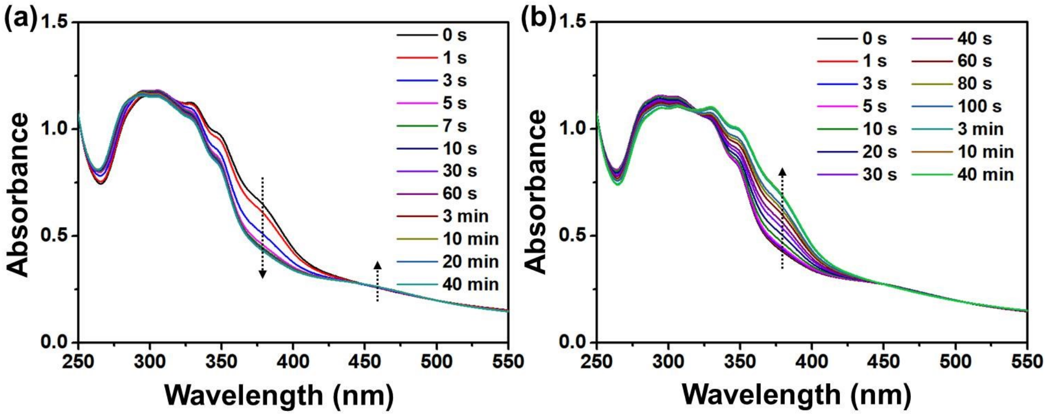

Fig. S15 UV-vis spectra of the assemblies for SCJNPs prepared from PPEGMA$_{14}$-*b*-P(MAAz$_{37}$-*co*-MAStb$_{72}$) in aqueous dispersion irradiated by (a) 360 nm UV light and (b) 520 nm visible light. For (b), 0 s is the spectrum after 360 nm UV irradiation for 40 min.

References

(1) W. Wen, T. Huang, S. Guan, Y. Zhao and A. Chen, *Macromolecules*, 2019, 52, 2956-2964.

(2) F. Zhou, M. Xie and D. Chen, *Macromolecules*, 2013, 47, 365-372.

(3) W. Fan, X. Tong, Q. Yan, S. Fu and Y. Zhao, *Chem. Commun.*, 2014, 50, 13492-13494.